Neuropharmacology 182 (2021) 108401

Contents lists available at ScienceDirect

Neuropharmacology

journal homepage: www.elsevier.com/locate/neuropharm

Chronobiotic effect of melatonin in experimental optic neuritis

Marcos L. Aranda [a], Omar Narvaez [b], Florencia Altschuler [a], Juan S. Calanni [a], María F. González Fleitas [a], Pablo H. Sande [a], Damián Dorfman [a], Luis Concha [b], Ruth E. Rosenstein [a,*]

[a] Laboratory of Retinal Neurochemistry and Experimental Ophthalmology, Department of Human Biochemistry, School of Medicine/CEFyBO, University of Buenos Aires/CONICET, Buenos Aires, Argentina
[b] Instituto de Neurobiología, Universidad Nacional Autónoma de México, Querétaro, Mexico

ARTICLE INFO

Keywords:
Optic neuritis
Non-image forming visual system
Melanopsin
Pupil light reflex
Locomotor activity
Melatonin

ABSTRACT

Optic neuritis (ON) is an inflammatory condition of the optic nerve, which leads to retinal ganglion cell (RGC) loss. A subset of RGCs expressing the photopigment melanopsin regulates non-image-forming visual system (NIFVS) functions such as pupillary light reflex (PLR) and circadian rhythms. Melatonin is a chronobiotic agent able to regulate the circadian system. We analyzed the effect of ON on the NIFVS, and the effect of melatonin on the NIFVS alterations induced by ON. For this purpose, optic nerves from male *Wistar* rats received vehicle or bacterial lipopolysaccharide (LPS), and one group of animals received a subcutaneous pellet of melatonin or a sham procedure. The NIFVS was analyzed in terms of: i) blue light-evoked PLR, ii) the communication between the retina and the suprachiasmatic nuclei (by anterograde transport, and *ex vivo* magnetic resonance images), iii) locomotor activity rhythm, and iv) Brn3a(+) and melanopsin(+) RGC number (by immunohistochemistry). Experimental ON significantly decreased the blue light-evoked PLR, induced a misconnection between the retina and the suprachiasmatic nuclei, decreased Brn3a(+) RGCs, but not melanopsin(+) RGC number. A bilateral injection of LPS significantly increased the light (but not dark) phase locomotor activity, rhythm periodicity, and time of offset activity. Melatonin prevented the decrease in blue light-evoked PLR, and locomotor activity rhythm alterations induced by ON. These results support that ON provoked alterations of the circadian physiology, and that melatonin could restore the circadian system misalignment.

1. Introduction

Optic neuritis (ON) involves optic nerve inflammation, demyelination, axon, and retinal ganglion cell (RGC) loss, and provokes ocular pain, abnormal visual acuity, color vision, pupillary light reflex (PLR), and visual evoked potentials (VEPs), which may worsen over 1–2 weeks, and usually begins improving over the next months. However, in ~40% of patients, visual disturbances (contrast sensitivity, color vision, PLR, and VEPs) remain permanent (Kaufman et al., 2000; Toosy et al., 2014). ON can be associated with neuromyelitis optica or multiple sclerosis (MS), and its validated rodent model, experimental autoimmune encephalomyelitis (EAE); however, the etiology for ON varies, including inflammation, infection, toxicity, and genetic disorders (Pau et al., 2011; Toosy et al., 2014). Acute ON often occurs as an isolated event, without systemic abnormalities, and considered idiopathic (or primary) (Toosy et al., 2014). We have developed an experimental model of primary ON induced by a microinjection of bacterial lipopolysaccharide (LPS) into the male *Wistar* rat optic nerve that replicates central features of human primary ON (Aranda et al., 2015). LPS provokes an early decrease in VEPs, and white light-induced PLR, optic nerve microglial/macrophage reactivity, and altered anterograde transport to the superior colliculus (SC), the lateral geniculate nucleus (LGN), and the olivary pretectal nucleus (OPN). Astrocytosis, demyelination, and axon, and RGC loss occur at 21 days post-LPS (Aranda et al., 2015). Melatonin restores

Abbreviations: CSD, constrained spherical deconvolution; CTB, cholera toxin β-subunit; DTI, diffusion tensor imaging; DWI, diffusion weighted images; EAE, experimental autoimmune encephalomyelitis; FA, fractional anisotropy; IFVS, image-forming visual system; ipRGCs, intrinsically photosensitive retinal ganglion cells; LGN, lateral geniculate nucleus; LPS, bacterial lipopolysaccharide; MS, multiple sclerosis; NIFVS, non-image-forming visual system; ON, optic neuritis; OPN, olivary pretectal nucleus; PLR, pupil light reflex; RGCs, retinal ganglion cells; SC, superior colliculus; SCN, suprachiasmatic nucleus; VEPs, visual evoked potentials.

* Corresponding author. Departamento de Bioquímica Humana, Facultad de Medicina/CEFyBO Universidad de Buenos Aires/CONICET Paraguay, 2155, 5°P (1121), Buenos Aires, Argentina.
E-mail address: ruthr@fmed.uba.ar (R.E. Rosenstein).

https://doi.org/10.1016/j.neuropharm.2020.108401
Received 17 July 2020; Received in revised form 6 November 2020; Accepted 9 November 2020
Available online 13 November 2020

VEPs, white light-induced PLR, and anterograde transport, and reduces microglial reactivity, astrocytosis, demyelination, and axon and RGC loss, induced by experimental ON (Aranda et al., 2016). Since ON-induced visual alterations can impair patients' abilities to perform daily activities, affecting life quality (Galetta et al., 2015), studies on ON have focused on conscious visual functions. However, the visual system consists of two major subsystems: i) the image-forming visual system (IFVS) that drives conscious vision, and ii) the non-image-forming visual system (NIFVS), which operates below the conscious perception level, regulating circadian photoentrainment, sleep/wake cycle, and PLR, among other functions (Chew et al., 2017). Most RGCs project to IFVS centers (i.e., the SC, and the LGN), whereas the information involved in NIFVS functions is carried out by a small subpopulation of RGCs that express the photopigment melanopsin, rendering them intrinsically photosensitive (ipRGCs) (Lucas et al., 2003; Panda et al., 2003). ipRGCs constitute the unique conduit of light information to NIFVS brain targets, such as the suprachiasmatic nucleus (SCN) (Hattar et al., 2003; Panda et al., 2003). Many light-regulated functions, including circadian clock entrainment, melatonin photic suppression, and PLR are retained in blind animals due to rod and cone degeneration in which there is a preservation of ipRGCs (Foster et al., 1991; Freedman et al., 1999; Lucas et al., 2001, 2003).

The post-illumination pupillary response has been used as an ipRGCs marker in optic neuropathies, including ON (Pau et al., 2011; Meltzer et al., 2017; Richter et al., 2017). However, NIFVS alterations within ON remain to be confirmed (Ba-Ali and Lund-Andersen, 2017). Herein, the influence of LPS-ON on the NIFVS was analyzed. Moreover, based on the well-known role of melatonin as a chronobiotic (Cajochen et al., 2003; Zisapel, 2018), we examined the effect of melatonin on the ON-induced NIFVS misalignment.

2. Materials and methods

2.1. Animals

All procedures concerning animals were in strict accordance with the Research Reporting of In-Vivo Experiments (ARRIVE) guidelines. The ethics committee of the School of Medicine, University of Buenos Aires (Institutional Committee for the Care and Use of Laboratory Animals, (CICUAL)) approved this study, and all efforts were made to minimize animal suffering. Male *Wistar* rats (300 ± 50 g) were housed in a standard animal room with food and water *ad libitum* under controlled conditions of temperature (21 ± 2 °C), luminosity (200 lux), and humidity, under a 12-h light/12-h dark lighting schedule (lights on at 8:00 a.m.). A total number of 57 animals was used for the experiments, distributed as follows: 10 animals for PLR studies, 5 animals for cholera toxin β-subunit (CTB) transport studies, 4 animals for diffusion tensor imaging, 8 animals bilaterally injected with vehicle or LPS for locomotor activity rhythm studies, 10 animals for immunohistochemical studies, and 20 animals for studying the effect of melatonin on PLR, and locomotor activity rhythms.

2.2. Experimental optic neuritis

To induce experimental ON, animals were anesthetized with ketamine hydrochloride (150 mg/kg) and xylazine hydrochloride (2 mg/kg) administered intraperitoneally. Animal's head was shaved and the skin was disinfected with povidone-iodine (Pervinox). A lateral canthotomy was made to perform an incision of 2–3 mm. Lacrimal glands and extraocular muscles were dissected to expose 3 mm of the retrobulbar optic nerve under a surgical microscope. The optic nerve sheaths were opened longitudinally and a microinjection was performed with a 30G needle attached to a Hamilton syringe (Hamilton, Reno, NV, USA). The needle was inserted into the optic nerve as superficially as possible, 2 mm posterior to the globe (i.e., the pre-chiasmatic region), and 1 μl of 4.5 μg/μl *Salmonella typhimurium* LPS (Sigma Chemical Co., St Louis, MO, USA) in pyrogen-free saline, was injected over approximately 10 s. In the present study, vehicle-injected optic nerve served as the control group because in a previous study we found that vehicle injection *per se* did not affect optic nerve function and histology (Aranda et al., 2015). After injection, the skin incision was sutured, and antibiotics were topically administered to prevent infection. In order to maximize functional and histological visual pathway damage, and to discard the possibility of a transient protection by melatonin, most of the experiments were performed at 21 days post-LPS. However, since at 21 days post-LPS there is a massive loss of optic nerve axons, we studied the effect of experimental optic neuritis on the functional communication between the retina and its main targets at 7 days post-LPS, assuming that functional alterations predate morphological changes.

2.3. Pupillary light reflex

Animals were dark-adapted for 2 h. The eye in which the optic nerve was injected with vehicle or LPS was stimulated with high intensity blue light (1 cm apart, 480 nm bandpass filter, 570 μW/cm^2) for 30 s, and the PLR was recorded in the contralateral (intact) eye (i.e., consensual PLR). The recordings were made at 21 days post-injection under infrared light with a digital video camera (Sony DCR-SR60, Tokyo, Japan), as previously described (Aranda et al., 2015, 2016; Fernandez et al., 2013). The sampling rate was 30 frames per second. Images were acquired with OSS Video Decompiler Software (One Stop Soft, New England, USA). The results were expressed as the percentage of the pupil contraction before (steady state) and 30 s after the light pulse.

2.4. Anterograde transport

In order to study the effect of experimental ON on anterograde transport from the retina to the SCN, we used 5 animals per group. At 18 days post-injection of vehicle or LPS, rats were anesthetized, and a drop of 0.5% proparacaine (Anestalcon, Alcon Laboratories, Buenos Aires, Argentina) was topically administered for local anesthesia. Using a 30G Hamilton syringe (Hamilton, Reno, NV, USA), 4 μl of 0.1% of cholera toxin β-subunit (CTB) conjugated to Alexa 488 or Alexa 568 dyes (Molecular Probes Inc., Eugene, OR, USA) in 0.1 mol/L PBS (pH 7.4) was injected into the vitreous, as previously described (Aranda et al., 2015, 2016). The injections were applied 1 mm from the limbus, and the needle was left in the eye for 30 s to prevent volume loss. After injection, antibiotics were topically administered to prevent infection. Three days after injection, rats were anesthetized and intracardially perfused. Brains were carefully removed, post-fixed overnight at 4 °C, and immersed in a graded series of sucrose solutions for cryoprotection; coronal sections (40 μm) from the SCN were obtained using a freezing microtome (CM 1850; Leica, Leica Microsystems, Buenos Aires, Argentina), mounted in glasses and viewed under an epifluorescence microscope (BX50, Olympus, Duarte, CA, USA).

2.5. Diffusion magnetic resonance imaging of the retinohypothalamic tract

Ex vivo magnetic resonance images (MRI) were acquired at the National Laboratory for MRI at the Universidad Nacional Autónoma de México, using a 7 T Bruker Pharmascan 70/16 scanner (Gmax = 760 mT/m). Animals were intracardially perfused with 4% paraformaldehyd and 2.5% glutaraldehyde with 0.2 mM Gadolinium (Gadovist, Bayer, Leverkusen, Germany) (D'Arceuil et al., 2007). Brains were extracted and placed in a plastic tube filled with perfluoropolyether (Fluorinert FC-70, Sigma-Aldrich, St. Louis, MO, USA). A helium-cooled surface radio-frequency coil was used for transmit and receive (Bruker Cryoprobe, Billerica, MA, USA), with the specimen's chiasm in close proximity to the coil. A segmented, three-dimensional echo-planar acquisition was used (8 segments, TR/TE = 250/25.19 ms cubic FOV of 11.52 mm per side (voxel size = 80 μm per side). After careful shimming,

twenty volumes without diffusion sensitization (b = 0 s/mm^2) were acquired, followed by diffusion weighted images (DWI) in four *shells* (b = 1000 s/mm^2, 20 directions; b = 3000 s/mm^2, 34 directions; b = 5000 s/mm^2, 52 directions; and b = 7000 s/mm^2, 54 directions. Diffusion gradient duration [δ] and separation [Δ] were kept constant at 4.9 and 10.84 ms, respectively. Total scanning time was 15 h. The DWI data sets were analyzed offline using MRtrix (version 3.0RC) and FSL tools (version 5.0.6). Pre-processing consisted on (i) denoising (Veraart et al., 2016), (ii) correction of Gibbs ringing (Kellner et al., 2016), (iii) correction of bias field inhomogeneities using the N4 algorithm (Tustison et al., 2010), estimated on the average non-diffusion weighted volume, and propagated to the entire data set, (iv) correction for eddy-current geometric distortions. The single-fiber response function was calculated with Dhollander's algorithm (Dhollander et al., 2016), and used to perform constrained spherical deconvolution (CSD) (Tournier et al., 2004). From this, the fiber orientation distribution was estimated. Probabilistic tractography was performed by seeding 1 million streamlines within a manually-defined region of interest in each optic nerve. Next, we used spherical deconvolution informed filtering of tractograms (Smith et al., 2013), which estimates the number of streamlines that are robustly supported by the underlying data. To quantify the changes in the fibers integrity, Diffusion Tensor Imaging (DTI) parameter fractional anisotropy (FA) was obtained. A selection of 332.1 ± 98.2 voxels in each optic nerve from 4 animals was used as regions of interest.

2.6. Effect of experimental ON on canonical and melanopsin(+) RGCs

In order to study the effect of experimental ON on canonical and melanopsin(+) RGCs, immunohistochemical studies on flat mount retinas were performed. At 21 days post-injection, animals were deeply anesthetized and intracardially perfused with saline, followed by a fixative solution (4% paraformaldehyde in PBS, pH 7.4). Eyeballs were carefully removed and corneas and lens were cut off. Eye-cups were post-fixed with 4% paraformaldehyde in 0.1 mol/L PBS (pH 7.4) for 30 min. Retinas were carefully detached and flat-mounted with the vitreous side up in superfrost microscope slides (Erie Scientific Company, Portsmouth, New Hampshire, USA). Whole-mount retinas were incubated overnight at 4 °C with a goat *anti*-Brn3a antibody (RRID: AB_2167511, 1:500; Santa Cruz Biotechnology, Buenos Aires, Argentina), and a rabbit polyclonal *anti*-melanopsin (PA1-780, 1:750, Affinity Bioreagent, Rockford, IL, USA) for 48 h. After several washes, a donkey anti-goat secondary antibody conjugated to Alexa 488 (A32814, 1:500; Molecular Probes, Buenos Aires, Argentina), and a donkey anti-rabbit secondary antibody conjugated to Alexa 568 (RRID: AB_2636995, 1:500; Molecular Probes, Buenos Aires, Argentina) were added, and incubated for 2 h at room temperature. Finally, retinas were mounted with fluorescent mounting medium (Dako, Glostrup, Denmark), and observed under an epifluorescence microscope (BX50; Olympus, Tokyo, Japan) connected to a video camera (3CCD; Sony, Tokyo, Japan), attached to a computer running image analysis software (Image-Pro Plus, Media Cybernetics Inc., Bethesda, USA). For each retina, results obtained from eight separate quadrants (four from the center and four from the periphery) were averaged, and the mean of 5 eyes was recorded as the representative value. Immunofluorescence studies were performed by analyzing comparative digital images from different samples, and by using identical exposure time, brightness, and contrast settings. All the images obtained were assembled and processed using Adobe Photoshop CS5 (Adobe Systems, San Jose, CA, USA) to adjust brightness and contrast. No other adjustments were made. For all morphometric image processing and analysis, digitalized captured TIFF images were transferred to ImageJ software (National Institutes of Health, Bethesda, Maryland; http://imagej.nih.gov/ij/).

2.7. Melatonin administration

A group of 20 rats was subcutaneously implanted with a pellet of melatonin (Sigma Chemical Co., St Louis, MO, USA, 20 mg with 3% w/v vegetable oil), compressed in a bronze cylinder of 2.5 mm diameter and 1 mm length), while a control group was sham-operated without the pellet implant. The pellet of melatonin was implanted 1 day before vehicle or LPS injection, and was replaced every 10 days. The administration procedure and dose of melatonin were selected on the basis of previous reports (Aranda et al., 2016; Belforte et al., 2010; Sande et al., 2008). As already mentioned, the effect of melatonin was assessed at 21 days post-LPS.

2.8. Locomotor activity rhythms

Daily rhythms of locomotor activity were registered under 12 h light (200 lux)/12 h dark cycles, as previously described (Fernandez et al., 2013; González Fleitas et al., 2015). Animals were bilaterally injected with vehicle or LPS. In another set of experiments, animals bilaterally injected with vehicle or LPS were submitted to a sham procedure or melatonin treatment. After recovery from anesthesia, animals were placed in cages equipped with infrared detectors of motion. Data were sampled every 5 min and stored for subsequent analysis during 15 days, before and 21 days after vehicle or LPS injection. Double-plot actograms, periodograms and average activity waveforms were built with ActogramJ (Image J, National Institutes of Health, Bethesda, Maryland, USA; http://imagej.nih.gov/ij/). Average activity during the light and dark phases, periodicity, and activity onset and offset Zeitgeber time were calculated.

2.9. Data and statistical analysis

Experimenters were blinded to group assignment and outcome assessment for all experiments, and all involved observers. The optimum sample sizes and animal numbers were determined by power analysis of pre - existing data. Animals were assigned randomly to various experimental groups (using a random number generator: http://www.randomizer.org/form.htm). The data collected were processed randomly and appropriately blocked. The declared group size is the number of independent values. Normality was assessed by Shapiro-Wilks test. Grubb's test was performed in order to detect outliers. No outliers were detected. Statistical analysis of results was performed by Student's *t*-test or two-way analysis of variance (ANOVA), followed by Tukey's test. Significance was set at *P* values below 0.05 for all analyses, and values are expressed as mean ± standard error (SE). Programs used in all cases were Prism 6.1 for Windows (GraphPad Software Inc., San Diego, CA, USA) and InfoStat for Windows (version 2018, URL http://www.infostat.com.ar, Cordoba, Argentina). The data and statistical analysis comply with the recommendations of the British Journal of Pharmacology on experimental design and analysis in pharmacology (Curtis et al., 2018).

3. Results

3.1. Effect of optic neuritis on PLR

In order to assess the effect of experimental ON on the NIFVS function, the blue-light induced PLR was examined at 21 days post-injection in animals in which one optic nerve was injected with vehicle or LPS, and the contralateral optic nerve remained intact. When eyes whose optic nerves were injected with LPS were stimulated with blue light, a significant decrease in the pupil contraction magnitude in the contralateral intact eye was observed, as shown in Fig. 1 ($t(4.94) = 3.42$, $p = 0.0115$).

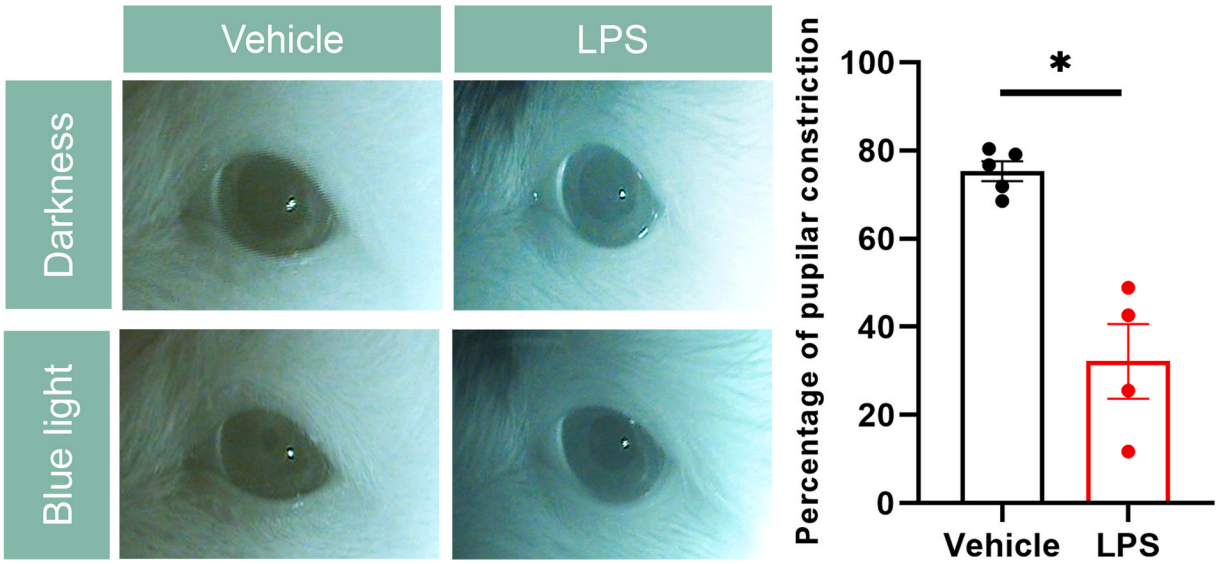

Fig. 1. Effect of LPS on blue light-evoked PLR. Left panel: Representative images of the consensual PLR induced by blue light in an animal in which one optic nerve was injected with vehicle or LPS and the contralateral optic nerve remained intact, at 21 days post-injection. Right panel: The pupil diameter (relative to the limbus diameter) was measured, and the percentage of pupil constriction was calculated in the contralateral eye whose optic nerve remained intact. LPS induced a significant decrease in the average of pupillary constriction in response to a blue light flash (1200 lux). Data are the mean ± SEM (n = 5 eyes per group). *$P < 0.05$ vs. vehicle, by Student's *t*-test.

3.2. Locomotor activity rhythm

Locomotor activity rhythms were recorded in animals that received vehicle or LPS in both optic nerves. Fig. 2 shows representative actograms (Fig. 2A), periodograms (Fig. 2B), and average activity waveforms (Fig. 2C) for vehicle- or LPS-treated rats. Animals that received LPS in both optic nerves were significantly more active during the light ($t(2.71) = 5.67$, $p = 0.0369$) (but not dark) phase than control animals ($t(0.34) = 4.31$, $p = 0.74$) (Fig. 3A). Moreover, bilateral ON induced a significant increase in periodicity ($t(3.16) = 3.66$, $p = 0.0386$) (Fig. 3B), and the Zeitgeber time of activity offset ($t(3.50) = 5.97$, $p = 0.0129$) (Fig. 3C). No differences in the activity onset time were observed between groups (data not shown).

3.3. Retinal anterograde transport

In order to analyze the retinohypothalamic track, the active anterograde transport from RGCs to the SCN, CTB conjugated to Alexa 568 dye (red) and CTB conjugated with Alexa 488 dye (green) were intravitreally injected in eyes whose optic nerves were injected with vehicle or LPS, respectively. Experimental ON induced a clear reduction in CTB staining in the SCN (Fig. 4). DTI images revealed dense connections from the intact optic nerve reaching the contralateral SCN, or coursing through the contralateral optic tract. In contrast, there was a paucity of connections arising from the injured optic nerve to the SCN, or traversing through the optic tract (Fig. 4D). FA was quantified as a directional diffusion parameter from DTI (taking values from zero (isotropic) to one (anisotropic)). LPS induced a significant reduction in the retinohypothalamic tract FA values in comparison to controls ($t(3) = 7.56$, $p = 0.0048$) (Fig. 4E).

3.4. Analysis of canonical and melanopsin expressing RGC number

Brn3a is a POU domain transcription factor specifically expressed in canonical (but not melanopsin expressing) RGCs (Nadal-Nicolás et al., 2012). Fig. 5 shows melanopsin- and Brn3a-immunoreactivity in flat-mounted retinas from eyes whose optic nerves were injected with vehicle or LPS, at 21 days post-injection. The injection of LPS into the optic nerve induced a significant decrease in Brn3a(+) RGC ($t(7.88) = 7.91$, $p = 0.001$), but not in melanopsin(+) RGC number ($t(0.80) = 7.99$, $p = 0.44$).

3.5. Effect of melatonin on NIFVS alteration

In order to analyze the effect of melatonin on the NIFVS alterations induced by experimental ON, a group of animals received a subcutaneous pellet of melatonin or a sham procedure, and the PLR, and locomotor activity daily rhythms were assessed. Melatonin treatment prevented the decrease in blue light-evoked PLR induced by ON ($F(2,12) = 13.57$; $p = 0.0008$) (Fig. 6). Fig. 7 shows periodograms (upper panel), and average activity waveforms (lower panel) from sham-operated or melatonin-treated animals which received vehicle or LPS into both optic nerves. Melatonin, which induced *per se* an increase in the locomotor activity during the dark phase ($F(3,16) = 3.76$; $p = 0.0324$), significantly prevented the alterations in the locomotor activity during the light phase ($F(3,16) = 8.95$; $p = 0.001$), periodogram ($F(3,16) = 5.10$; $p = 0.011$), and time of activity offset ($F(3,16) = 4.66$; $p = 0.0159$) induced by ON (Fig. 8).

4. Discussion

The present results demonstrate that LPS-ON provoked significant alterations in the NIFVS functions that were prevented by melatonin. Although recent findings suggest a much broader involvement of the NIFVS in a complex array of light-induced physiologic responses, classical functions associated to this system include PLR, and sleep/wake cycles (Hughes et al., 2016; Ksendzovsky et al., 2017). The blue light-induced PLR represents a potentially important neurophysiologic signature for ipRGC integrity in humans (Meltzer et al., 2017). In agreement with results from ON patients (Meltzer et al., 2017; Richter et al., 2017), LPS-ON decreased the blue light-evoked PLR. A small population of ipRGCs (2%–3% of all ipRGCs) projects into the OPN for the coordination of melanopsin-mediated PLR (Chew et al., 2017). We have shown that LPS-ON diminishes the anterograde transport to the OPN (Aranda et al., 2015) which could account for the decreased blue light-evoked PLR.

To further analyze the NIFVS functions, we recorded general activity daily patterns in animals in which both optic nerves received vehicle or

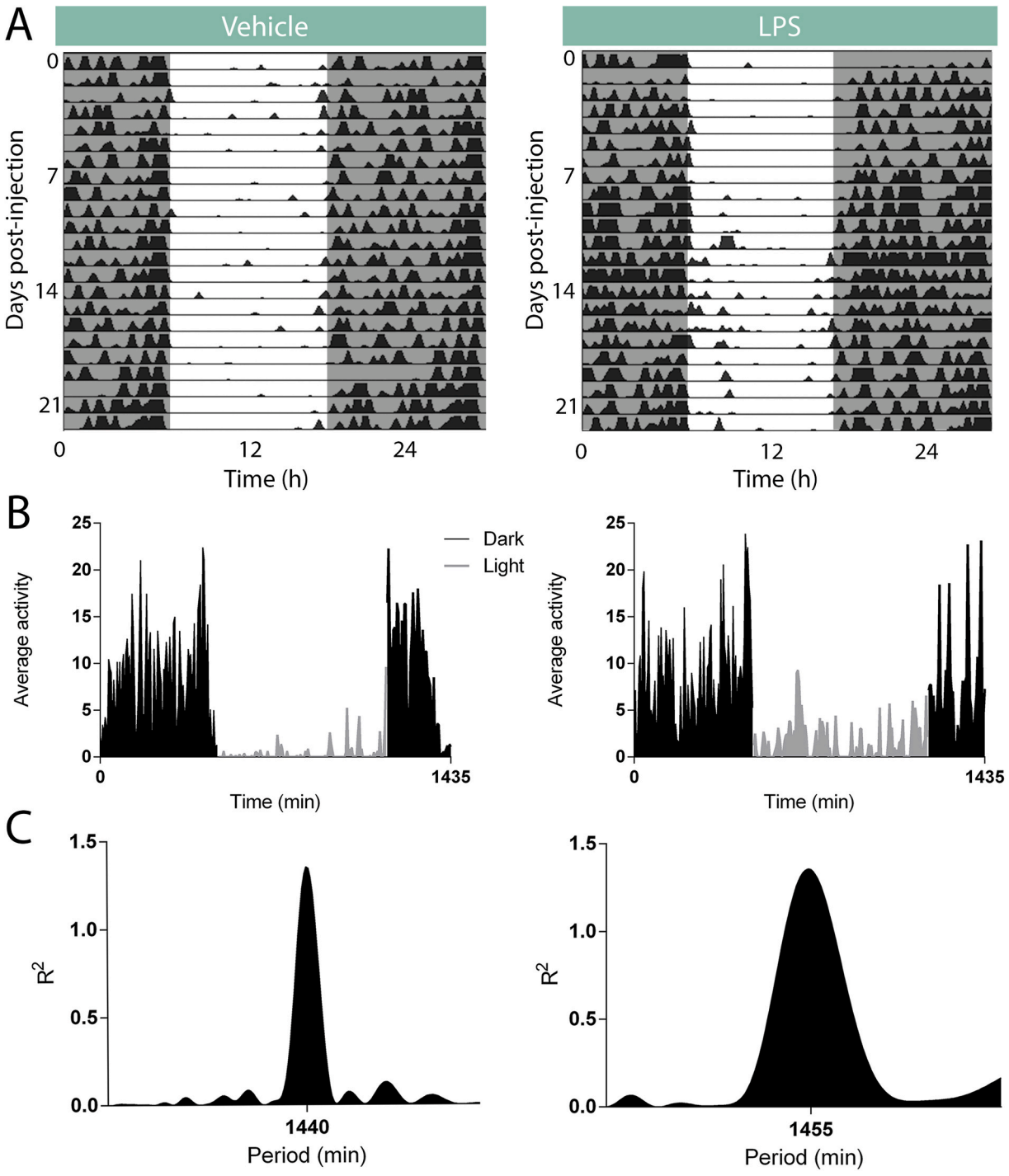

Fig. 2. Locomotor activity rhythms from animals bilaterally injected with vehicle or LPS into the optic nerve. Panel A: Representative double-plotted actograms at 21 days post-injection of vehicle or LPS, under a normal L:D cycle. Panel B: Representative periodograms from vehicle- (left) or LPS- (right) injected animals. Panel C: Representative activity phase waveforms from vehicle- (left) or LPS- (right) injected animals.

LPS. Bilateral ON increased the locomotor activity rhythm periodicity, and the time of activity offset. As expected for nocturnal animals under artificial lighting conditions, control rats showed very low activity during the light phase, whereas bilateral ON significantly increased locomotor activity in the light (but not dark) phase. Despite the well-known differences between humans and rats, the alterations in the light phase activity in animals with bilateral ON (higher activity during the rest (i.e., light) phase), could suggest a sleep/wake rhythm disturbance in human ON. In agreement, the majority of individuals with MS suffers from sleep disorders (Chinnadurai et al., 2018; Najafi et al., 2013), and sleep/wake rhythm disturbances have been demonstrated in EAE mice (He et al., 2014).

An alteration in light transmission from the retina to the SCN may result from retinal and/or optic nerve injury. To analyze the retinohypothalamic tract, CTB was intravitreally injected in eyes whose optic nerves were injected with vehicle or LPS. In contrast to the retinal projections to IFVS targets in rodents that primary arise *via* the contralateral hemisphere, the SCN receives dense bilateral retinal innervation, with only a slight contralateral dominance (Morin and Studholme, 2014). LPS injection induced a deficit in CTB anterograde transport to

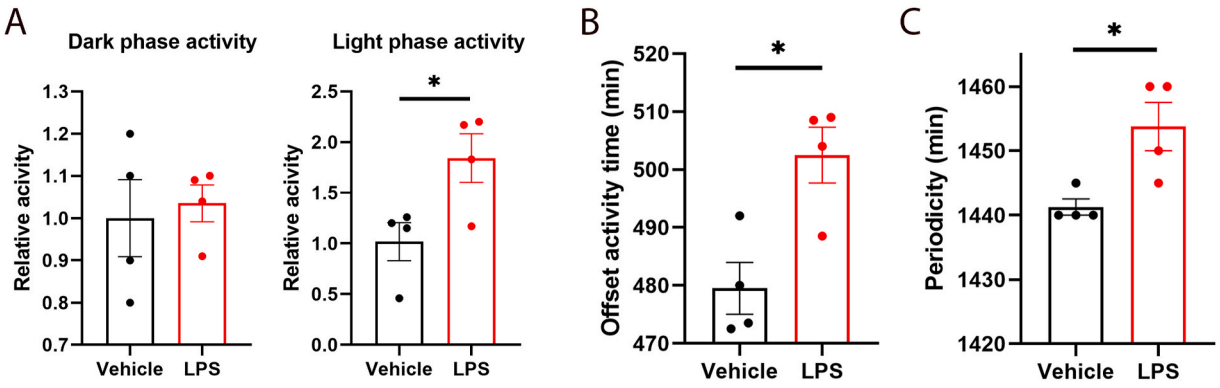

Fig. 3. Effect of experimental ON on locomotor activity in dark and light phases, periodicity and offset activity time. Panel A: quantification of dark (left) and light (right) phase activity from vehicle- or LPS-injected animals. Animals that received LPS in both optic nerves were significantly more active during the light (but not dark) phase than control animals. Panel B: quantification of periodicity. Bilateral ON induced a significant increase in the periodicity. Panel C: quantification of the offset activity time. Bilateral LPS-injected animals showed a significant increase in this parameter. Data are the mean ± SEM (n = 4 animals/group). *$P < 0.05$ vs. vehicle, by Student's *t*-test.

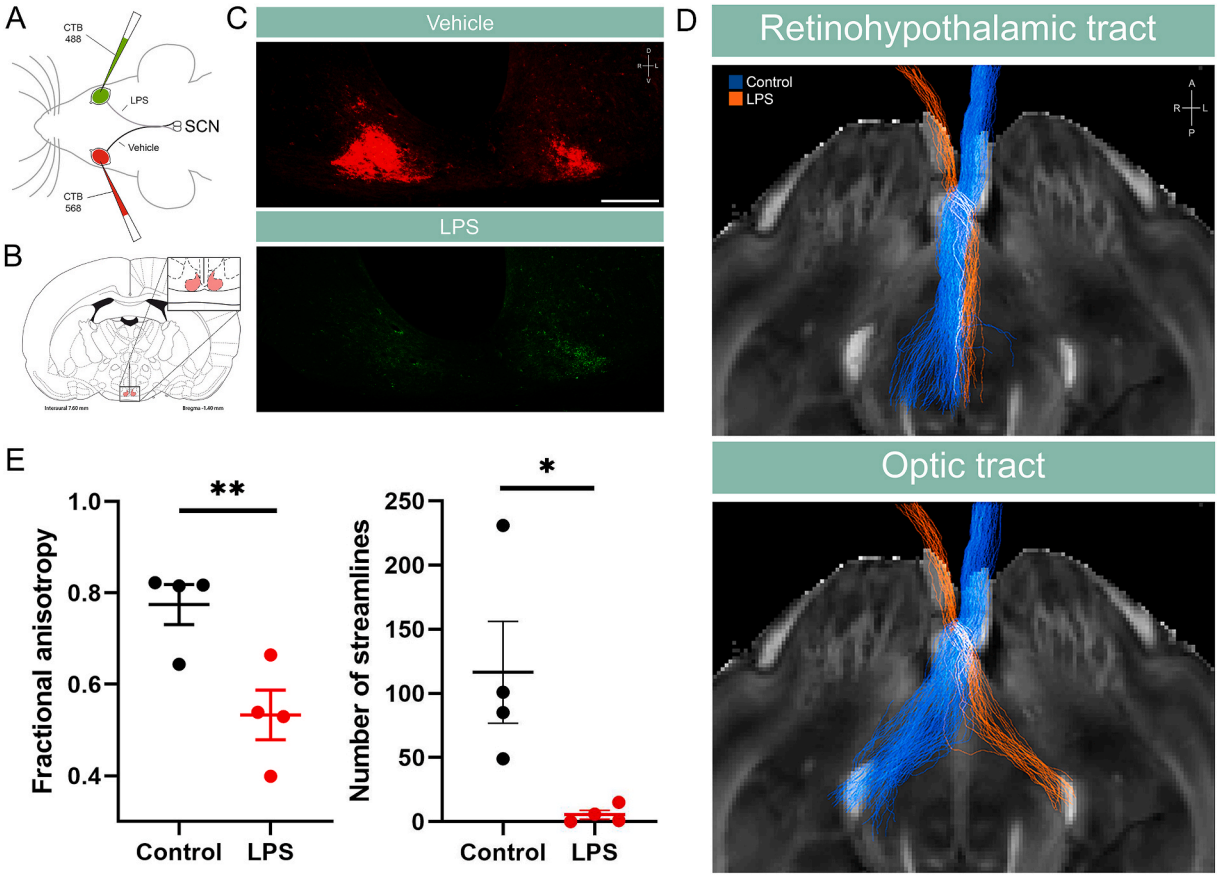

Fig. 4. Anterograde transport from the retina to the SCN, and *ex vivo* MRI analysis of the retinohypothalamic and the optic tract. Panel A: CTB conjugated to Alexa 586 (red) was injected in the vitreous from eyes whose optics nerves were injected with vehicle, and CTB conjugated to Alexa 488 (green) was injected into the vitreous from eyes whose optics nerves received LPS. Panel B: schematic localization of SCN (Paxinos and Watson, 1997). Panel C: representative photomicrographs of SCN sections (n = 5 per group). At 21 days post-injection, LPS induced a clear reduction of the retinal terminal density in the ipsi and contralateral SCN. Panel D: Tractography of the optic nerves injected with vehicle (blue), or LPS (orange), showing streamlines traversing to both the contralateral optic and retinohypothalamic tracts at 7 days post-injection of LPS. Panel E: quantification of fractional anisotropy (FA) diffusion tensor image parameter from control or LPS injected tracts. LPS injected tracts showed reduced FA values in comparison to controls. Data are mean ± SEM (n = 4 animals per group), **$P < 0.01$, by paired Student's *t*-test.

both ipsi- and contralateral SCN, supporting that LPS-ON caused a deficient communication between the retina and the master circadian pacemaker. This hypothesis was supported by tractography, a method used to indirectly assess structural connectivity. The reduced number of streamlines that reach their targets is a reflection of the altered microstructural environment of the affected optic nerve, thereby modulating its water diffusion profile. We have shown that ON decreases CTB anterograde transport from the retina to the SC, and the LGN (the main retinal synaptic targets in the rodent IFVS) (Aranda et al., 2015), which was confirmed herein by MRI analysis of the optic tract.

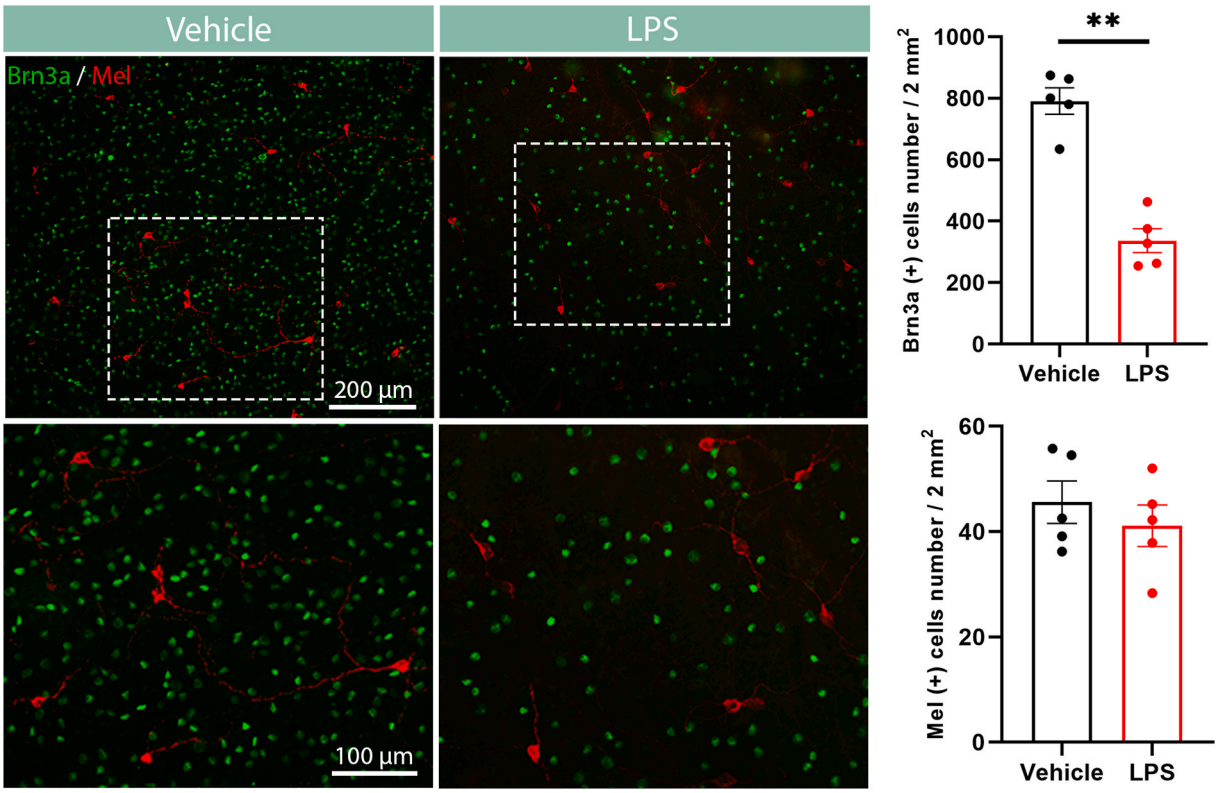

Fig. 5. Effect of experimental ON on Brn3a(+) RGCs and melanopsin(+) RGCs. Left panel: Shown are representative photomicrographs of double immunostaining against Brn3a (green) and melanopsin (red) in flat-mounted retinas from animals whose optic nerves were injected with vehicle (left) or LPS (right). Higher magnification pictures are shown in the bottom. Right panel: Quantification of Brn3a(+) and melanopsin(+) cells, at 21 days post-injections into the optic nerve. In retinas from eyes whose optic nerves were injected with LPS, a significant decrease in the number of Brn3a(+) cells was observed, whereas melanopsin(+) RGC number did not differ between groups. Data are mean ± SEM (n = 5 animals per group), $^{**}P < 0.01$, by Student's *t*-test.

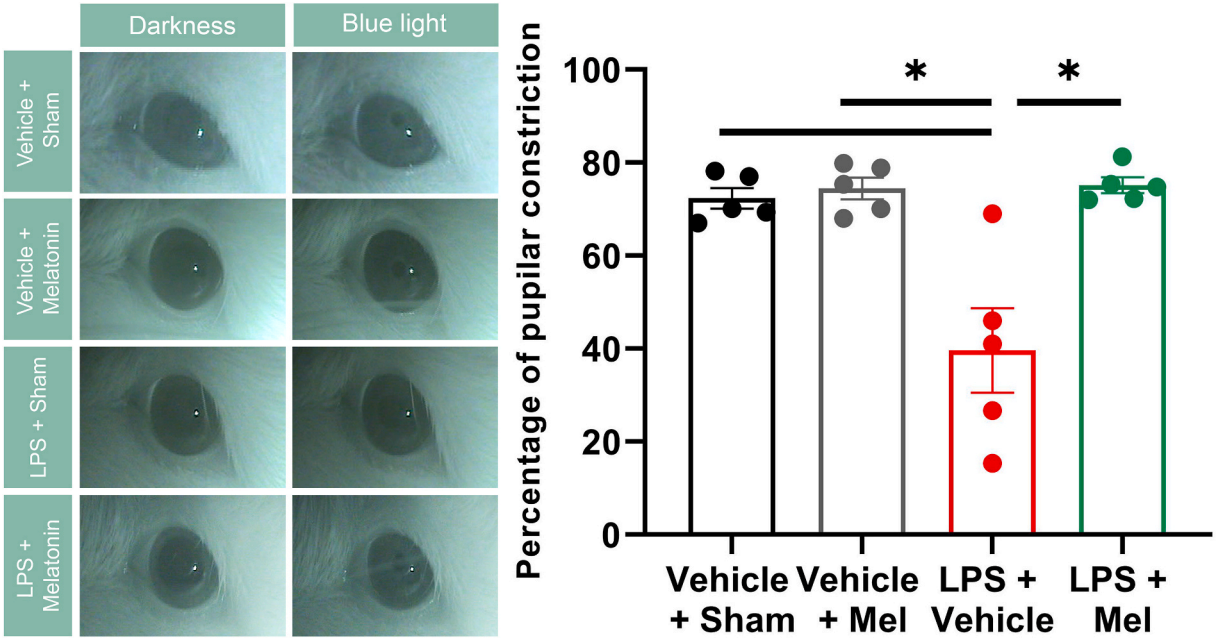

Fig. 6. Effect of melatonin on the alterations in PLR induced by ON. Left panel: Representative images of the consensual PLR induced by blue light in an animal in which one optic nerve was injected with vehicle and was submitted to sham treatment; an animal which received vehicle and was implanted with a subcutaneous pellet of melatonin; an animal which received LPS into the optic nerve and a sham treatment; and an animal which received LPS into the optic nerve and a subcutaneous pellet of melatonin. The contralateral optic nerve remained intact in all these groups. Right panel: Melatonin prevented the effect of LPS on the blue light-evoked PLR. Data are the mean ± SEM (n = 5 eyes per group). $^{*}P < 0.05$, by Tukey's test.

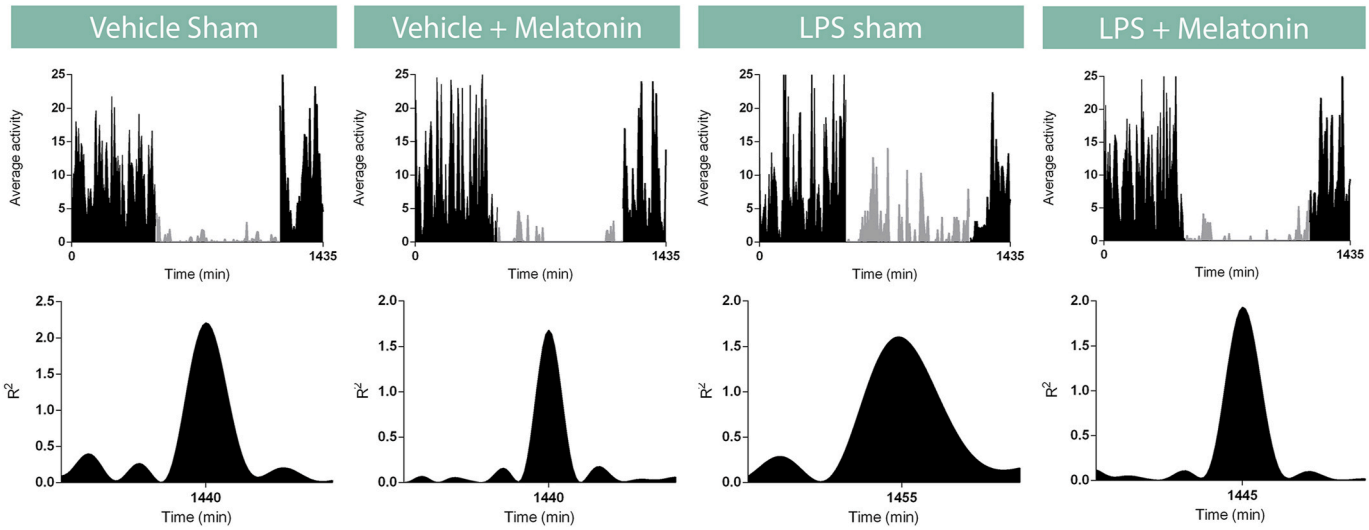

Fig. 7. Effect of melatonin on locomotor activity rhythms alterations induced by experimental ON. Representative periodograms (upper panel) and average activity waveforms (bottom panel) from animals bilaterally injected with vehicle or LPS, in the presence or absence of melatonin (n = 5 animals per group).

Taken together, these results suggest that axons projecting to IFVS and NIFVS areas could be similarly vulnerable to the damaging effect of optic nerve inflammation.

To analyze the retinal contribution to the effect of ON on the NIFVS, the number of melanopsin(+) RGCs was analyzed. At an advanced stage of ON (i.e., at 21 days post-LPS), concomitantly with a significant Brn3a (+) RCG loss, a preservation of ipRGC number occurred in the retina from LPS-injected optic nerves. Although we did not ascertain whether ipRGC number still persists at later stages, our results showed that melanopsin(+) RGCs were more resilient than canonical RGCs to damage induced by LPS-ON. It should be noted that as in almost all of the studies to date on ipRGCs in injury models or pathological conditions, our results mostly reflect M1 ipRGCs that express high levels of melanopsin and are thus easily identified (Cui et al., 2015). Therefore, we cannot still establish the effect of ON on other ipRGC types that express much lower melanopsin levels (M2-M6) (Cui et al., 2015). The ipRGC resistance to different damaging conditions has been intensively studied (Ba-Ali and Lund-Andersen, 2017; Cui et al., 2015). Animal models mimicking other optic nerve injuries, including optic nerve transection or crush, have shown that ipRGCs are more resilient compared to classical RGCs (Robinson and Madison, 2004; Sánchez-Migallón et al., 2018). Moreover, ipRGCs and the NIFVS are protected against acute retinal ischemic damage (González Fleitas et al., 2015), and at advanced stages of diabetic retinopathy (Fernandez et al., 2013). The ipRGC robustness has also been shown in patients with Leber's hereditary optic neuropathy, or dominant optic atrophy (La Morgia et al., 2010; Moura et al., 2013), and after exposing rodent retinas to NMDA (DeParis et al., 2012). In contrast, several lines of evidence strongly support that experimental and human glaucoma decrease the number of melanopsin (+) RGCs, and provokes significant alterations of the NIFVS function (Ba-Ali and Lund-Andersen, 2017; de Zavalía et al., 2011; Drouyer et al., 2008; Kankipati et al., 2011; Lanzani et al., 2012; Obara et al., 2016; Pérez-Rico et al., 2010). So far, to our knowledge, studies aimed at analyzing the influence of visual diseases on the NIFVS show a close correlation between the number of melanopsin expressing RGCs and the NIFVS function, in which ipRGC resilience or loss (mostly assessed by melanopsin-immunoreactivity) occur concomitantly with preservation or alteration of NIFVS functions, respectively. In that context, the present results support that ON could constitute a new scenario in which a preservation of ipRGC number coexisted with alterations in several functions of the NIFVS, and support that ON could be a key model that needs to be further investigated in regard to circadian photoreception in optic neuropathies. In addition, these results support that the retinohypothalamic track could be the anatomical locus of LPS-induced alterations of the NIFVS, at least at this stage of ON. Taken together, the present results support NIFVS function disturbances in experimental ON.

It has been clearly demonstrated that melatonin plays a key role in regulating circadian rhythms (Cajochen et al., 2003; Gordon, 2000; Touitou and Bogdan, 2007; Zisapel, 2018). Several reports have shown that melatonin has both hypnotic and chronobiotic properties that influence circadian rhythmicity, and avoid rhythm sleep/wake disorders (Li et al., 2019; van Geijlswijk et al., 2010; Wirz-Justice and Armstrong, 1996). Externally applied melatonin is used in humans as a chronobiotic drug to treat desynchronization and circadian disorders, supporting a pivotal role of melatonin in the circadian system synchronization (Pfeffer et al., 2018). Furthermore, it has been shown that melatonin can improve the reduced sleep quality in MS patients (Adamczyk-Sowa et al., 2014). Notably, levels of sleep mediators such as melatonin and orexin-A are reduced during the course of MS (Gencer et al., 2019; Türkoğlu et al., 2020), and it has been postulated that reduction of orexin-A and melatonin levels might be one of the underlying mechanisms involved in increased daytime sleepiness in MS patients (Türkoğlu et al., 2020).

To reach a continuous dosing and reducing animal manipulation as with a daily administration, and because in previous reports we showed the success of this dosing and administration procedure to achieve retinal and optic nerve protection of the IFVS in experimental ON (Aranda et al., 2016), melatonin was administered as subcutaneous pellets. The present results support that melatonin protected the NIFVS functions against LPS-ON, as shown by the preservation of the blue light-induced PLR, and the locomotor activity rhythm. Notably, melatonin *per se* (but not in animals that received LPS into the optic nerve), increased the locomotor activity during the dark-phase, at which endogenous melatonin levels are supposed to be higher than at the light-phase. In agreement, it has been shown that melatonin administration increases nocturnal (but not diurnal) locomotor activity in male *Wistar* rats (Terrón et al., 2013). However, in contrast to our findings, it has been demonstrated that interaperitoneally injected, melatonin inhibits locomotor activity in hamsters (Golombek et al., 1991), and that a subcutaneous injection of melatonin inhibits movement in house sparrows and Japanese quails (Murakami et al., 2001). At present, we have no explanation for this discrepancy; however, it seems that differences in doses, administration method, and species could account for it.

The mechanisms involved in melatonin-induced protection remain to be established. We have shown that melatonin prevents optic nerve axon loss induced by ON, likely through anti-inflammatory and/or

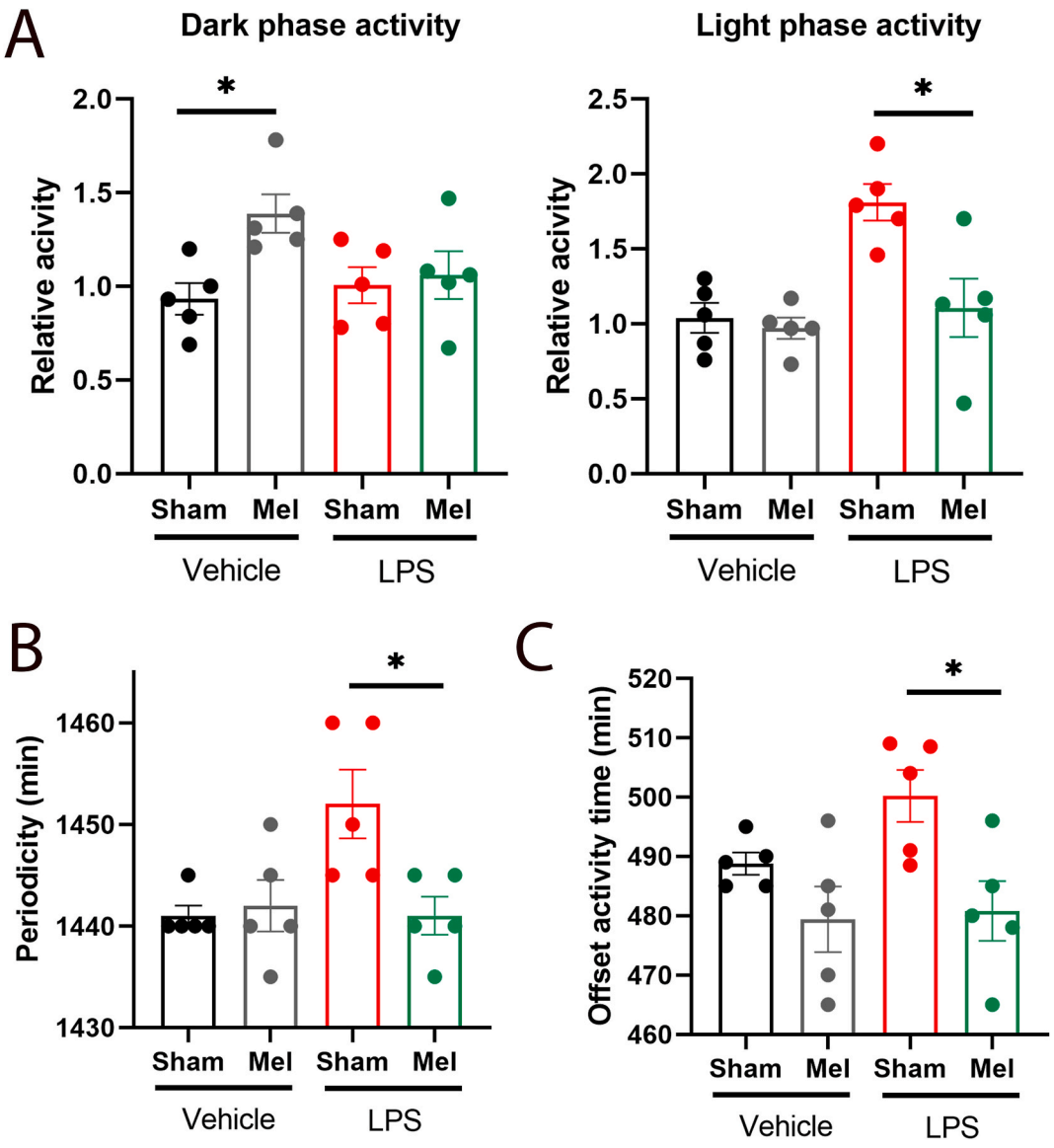

Fig. 8. Effect of melatonin on the locomotor activity during the dark and light phase, periodograms and the offset activity time alterations induced by experimental ON. Panel A: quantification of dark (left) and light (right) phase activity from vehicle- or LPS- injected animals in the presence or absence of melatonin. Melatonin, which induced *per se* an increase in the locomotor activity during the dark phase, significantly prevented the alterations in this parameter during the light phase induced by experimental ON. Panel B: Quantification of periodicity. Melatonin prevented the increase in periodicity induced by experimental ON. Panel C: Assessment of offset activity time. The increase in offset activity time induced by experimental ON was prevented by melatonin. Data are the mean ± SEM (n = 5 animals per group). *$P < 0.05$, by Tukey's test.

antioxidant effects (Aranda et al., 2016). Therefore, it seems possible that the same mechanisms could account for the protection of NIFVS axons. Currently, experiments aimed at studying the effect of melatonin on the retinohypothalamic tract are in progress.

5. Conclusions

ON may affect the life quality in several ways (Galetta et al., 2015), including the visual consequences of the disease itself, the psychological effects of diagnosis, the potential side effects of treatment, and financial effects (as the cost of visits and therapy). The present results suggest another risk to the life quality of ON patients, i.e., alterations of the circadian physiology. Circadian dysfunction can play a role in a wide range of pathologies, including sleep problems, impaired performance, decrease in cognitive skills, poor psychomotor coordination, and headaches, among many others (Abbott et al., 2020), prompting the need for therapeutic strategies to restore circadian balance in ON. In this line, the present results support that melatonin, therapeutically targeting both the IF (Aranda et al., 2016) and the NIFVS, could be a promissory resource in ON treatment.

CRediT authorship contribution statement

Marcos L. Aranda: Investigation, Conceptualization, Methodology, Formal analysis, Writing - original draft, All authors have approved the final version of this article. **Omar Narvaez:** Methodology, Investigation, Formal analysis, Writing - review & editing, All authors have approved the final version of this article. **Florencia Altschuler:** Methodology, Investigation, Formal analysis, All authors have approved the final version of this article. **Juan S. Calanni:** Methodology, Investigation, All authors have approved the final version of this article. **María F. González Fleitas:** Methodology, Investigation, Formal analysis, Writing - review & editing, All authors have approved the final version of this article. **Pablo H. Sande:** Methodology, Investigation, All authors have

approved the final version of this article. **Damián Dorfman:** Writing - original draft, All authors have approved the final version of this article. **Luis Concha:** Formal analysis, All authors have approved the final version of this article, Investigation, Conceptualization, Methodology. **Ruth E. Rosenstein:** Investigation, Conceptualization, Methodology, Writing - original draft, Writing - review & editing, All authors have approved the final version of this article.

Declaration of competing interest

None.

Acknowledgments

This research was supported by grants from the Agencia Nacional de Promoción Científica y Tecnológica [PICT 1563, PICT 2731]; The University of Buenos Aires [20020100100678]; Consejo Nacional de Investigaciones Científicas y Técnicas [PIP 1911], Argentina. The funding organizations have no role in the design or conduct of this research.

References

Abbott, S.M., Malkani, R.G., Zee, P.C., 2020. Circadian disruption and human health: a bidirectional relationship. Eur. J. Neurosci. 51, 567–583. https://doi.org/10.1111/ejn.14298.

Adamczyk-Sowa, M., Pierzchala, K., Sowa, P., Mucha, S., Sadowska-Bartosz, I., Adamczyk, J., Hartel, M., 2014. Melatonin acts as antioxidant and improves sleep in MS patients. Neurochem. Res. 39, 1585–1593. https://doi.org/10.1007/s11064-014-1347-6.

Aranda, M.L., Dorfman, D., Sande, P.H., Rosenstein, R.E., 2015. Experimental optic neuritis induced by the microinjection of lipopolysaccharide into the optic nerve. Exp. Neurol. 266, 30–41. https://doi.org/10.1016/j.expneurol.2015.01.010.

Aranda, M.L., González Fleitas, M.F., De Laurentiis, A., Keller Sarmiento, M.I., Chianelli, M., Rosenstein, R.E., 2016. Neuroprotective effect of melatonin in experimental optic neuritis in rats. J. Pineal Res. 60, 360–372. https://doi.org/10.1111/jpi.12318.

Ba-Ali, S., Lund-Andersen, H., 2017. Pupillometric evaluation of the melanopsin containing retinal ganglion cells in mitochondrial and non-mitochondrial optic neuropathies. Mitochondrion 36, 124–129. https://doi.org/10.1016/j.mito.2017.07.003.

Belforte, N.A., Moreno, M.C., de Zavalía, N., Sande, P.H., Chianelli, M.S., Keller Sarmiento, M.I., Rosenstein, R.E., 2010. Melatonin: a novel neuroprotectant for the treatment of glaucoma. J. Pineal Res. 48, 353–364. https://doi.org/10.1111/j.1600-079X.2010.00762.x.

Cajochen, C., Kräuchi, K., Wirz-Justice, A., 2003. Role of melatonin in the regulation of human circadian rhythms and sleep. J. Neuroendocrinol. 15, 432–437. https://doi.org/10.1046/j.1365-2826.2003.00989.x.

Chew, K.S., Renna, J.M., McNeill, D.S., Fernandez, D.C., Keenan, W.T., Thomsen, M.B., Ecker, J.L., Loevinsohn, G.S., VanDunk, C., Vicarel, D.C., Tufford, A., Weng, S., Gray, P.A., Cayouette, M., Herzog, E.D., Zhao, H., Berson, D.M., Hattar, S., 2017. A subset of ipRGCs regulates both maturation of the circadian clock and segregation of retinogeniculate projections in mice. Elife 6, e22861. https://doi.org/10.7554/elife.22861.020.

Chinnadurai, S.A., Gandhirajan, D., Pamidimukala, V., Kesavamurthy, B., Venkatesan, S. A., 2018. Analysing the relationship between polysomnographic measures of sleep with measures of physical and cognitive fatigue in people with multiple sclerosis. Mult. Scler. Relat. Disord. 24, 32–37. https://doi.org/10.1016/j.msard.2018.05.016.

Cui, Q., Ren, C., Sollars, P.J., Pickard, G.E., So, K.F., 2015. The injury resistant ability of melanopsin-expressing intrinsically photosensitive retinal ganglion cells. Neuroscience 284, 845–853. https://doi.org/10.1016/j.neuroscience.2014.11.002.

Curtis, M.J., Alexander, S., Cirino, G., Docherty, J.R., George, C.H., Giembycz, M.A., Hoyer, D., Insel, P.A., Izzo, A.A., Ji, Y., MacEwan, D.J., Sobey, C.G., Stanford, S.C., Teixeira, M.M., Wonnacott, S., Ahluwalia, A., 2018. Experimental design and analysis and their reporting II: updated and simplified guidance for authors and peer reviewers. Br. J. Pharmacol. 175, 987–993. https://doi.org/10.1111/bph.14153.

D'Arceuil, H.E., Westmoreland, S., de Crespigny, A.J., 2007. An approach to high resolution diffusion tensor imaging in fixed primate brain. Neuroimage 35, 553–565. https://doi.org/10.1016/j.neuroimage.2006.12.028.

DeParis, S., Caprara, C., Grimm, C., 2012. Intrinsically photosensitive retinal ganglion cells are resistant to N-methyl-d-aspartic acid excitotoxicity. Mol. Vis. 18, 2814–2827.

de Zavalía, N., Plano, S.A., Fernandez, D.C., Lanzani, M.F., Salido, E., Belforte, N., Sarmiento, M.I., Golombek, D.A., Rosenstein, R.E., 2011. Effect of experimental glaucoma on the non-image forming visual system. J. Neurochem. 117, 904–914. https://doi.org/10.1111/j.1471-4159.2011.07260.x.

Dhollander, T., Raffelt, D., Connelly, A., 2016. Unsupervised 3-tissue response function estimation from single-shell or multi-shell diffusion MR data without a co-registered T1 image. In: ISMRM Workshop on Breaking the Barriers of Diffusion MRI, p. 5.

Drouyer, E., Dkhissi-Benyahya, O., Chiquet, C., WoldeMussie, E., Ruiz, G., Wheeler, L.A., Denis, P., Cooper, H.M., 2008. Glaucoma alters the circadian timing system. PloS One 3, e3931. https://doi.org/10.1371/journal.pone.0003931.

Fernandez, D.C., Sande, P.H., de Zavalía, N., Belforte, N., Dorfman, D., Casiraghi, L.P., Golombek, D., Rosenstein, R.E., 2013. Effect of experimental diabetic retinopathy on the non-image-forming visual system. Chronobiol. Int. 30, 583–597. https://doi.org/10.3109/07420528.2012.754453.

Foster, R.G., Provencio, I., Hudson, D., Fiske, S., De Grip, W., Menaker, M., 1991. Circadian photoreception in the retinally degenerate mouse (rd/rd). J. Comp. Physiol. A. 169, 39–50. https://doi.org/10.1007/bf00198171.

Freedman, M.S., Lucas, R.J., Soni, B., von Schantz, M., Muñoz, M., David-Gray, Z., Foster, R., 1999. Regulation of mammalian circadian behavior by non-rod, non-cone, ocular photoreceptors. Science 284, 502–504. https://doi.org/10.1126/science.284.5413.502.

Galetta, S.L., Villoslada, P., Levin, N., Shindler, K., Ishikawa, H., Parr, E., Cadavid, D., Balcer, L.J., 2015. Acute optic neuritis: unmet clinical needs and model for new therapies. Neurol. Neuroimmunol. Neuroinflamm. 2, e135. https://doi.org/10.1212/NXI.0000000000000135.

Gencer, M., Akbayır, E., Sen, M., Arsoy, E., Yılmaz, V., Bulut, N., Tüzün, E., Türkoğlu, R., 2019. Serum orexin-A levels are associated with disease progression and motor impairment in multiple sclerosis. Neurol. Sci. 40, 1067–1070. https://doi.org/10.1007/s10072-019-3708-z.

Golombek, D.A., Escolar, E., Cardinali, D.P., 1991. Melatonin-induced depression of locomotor activity in hamsters: time-dependency and inhibition by the central-type benzodiazepine antagonist Ro 15-1788. Physiol. Behav. 49, 1091–1097. https://doi.org/10.1016/0031-9384(91)90336-m.

González Fleitas, M.F., Bordone, M., Rosenstein, R.E., Dorfman, D., 2015. Effect of retinal ischemia on the non-image forming visual system. Chronobiol. Int. 32, 152–163. https://doi.org/10.3109/07420528.2014.959526.

Gordon, N., 2000. The therapeutics of melatonin: a paediatric perspective. Brain Dev. 22, 213–217. https://doi.org/10.1016/s0387-7604(00)00120-0.

Hattar, S., Lucas, R.J., Mrosovsky, N., Thompson, S., Douglas, R.H., Hankins, M.W., Lem, J., Biel, M., Hofmann, F., Foster, R.G., Yau, K.W., 2003. Melanopsin and rod-cone photoreceptive systems account for all major accessory visual functions in mice. Nature 424, 76–81. https://doi.org/10.1038/nature01761.

He, J., Wang, Y., Kastin, A.J., Pan, W., 2014. Increased sleep fragmentation in experimental autoimmune encephalomyelitis. Brain Behav. Immun. 38, 53–58. https://doi.org/10.1016/j.bbi.2014.02.005.

Hughes, S., Jagannath, A., Rodgers, J., Hankins, M.W., Peirson, S.N., Foster, R.G., 2016. Signalling by melanopsin (OPN4) expressing photosensitive retinal ganglion cells. Eye 30, 247–254. https://doi.org/10.1038/eye.2015.264.

Kankipati, L., Girkin, C.A., Gamlin, P.D., 2011. The post-illumination pupil response is reduced in glaucoma patients. Invest. Ophthalmol. Vis. Sci. 52, 2287–2292. https://doi.org/10.1167/iovs.10-6023.

Kaufman, D.I., Trobe, J.D., Eggenberger, E.R., Whitaker, J.N., 2000. Practice parameter: the role of corticosteroids in the management of acute monosymptomatic optic neuritis. Report of the Quality Standards Subcommittee of the American Academy of Neurology. Neurology 54, 2039–2044. https://doi.org/10.1212/wnl.54.11.2039.

Kellner, E., Dhital, B., Kiselev, V.G., Reisert, M., 2016. Gibbs-ringing artifact removal based on local subvoxel-shifts. Magn. Reson. Med. 76, 1574–1581. https://doi.org/10.1002/mrm.26054.

Ksendzovsky, A., Pomeraniec, I.J., Zaghloul, K.A., Provencio, J.J., Provencio, I., 2017. Clinical implications of the melanopsin-based non-image-forming visual system. Neurology 88, 1282–1290. https://doi.org/10.1212/WNL.0000000000003761.

La Morgia, C., Ross-Cisneros, F.N., Sadun, A.A., Hannibal, J., Munarini, A., Mantovani, V., Barboni, P., Cantalupo, G., Tozer, K.R., Sancisi, E., Salomao, S.R., Moraes, M.N., Moraes-Filho, M.N., Heegaard, S., Milea, D., Kjer, P., Montagna, P., Carelli, V., 2010. Melanopsin retinal ganglion cells are resistant to neurodegeneration in mitochondrial optic neuropathies. Brain 133, 2426–2438. https://doi.org/10.1093/brain/awq155.

Lanzani, M.F., de Zavalía, N., Fontana, H., Sarmiento, M.I., Golombek, D., Rosenstein, R. E., 2012. Alterations of locomotor activity rhythm and sleep parameters in patients with advanced glaucoma. Chronobiol. Int. 29, 911–919. https://doi.org/10.3109/07420528.2012.691146.

Li, T., Jiang, S., Han, M., Yang, Z., Lv, J., Deng, C., Reiter, R.J., Yang, Y., 2019. Exogenous melatonin as a treatment for secondary sleep disorders: a systematic review and meta-analysis. Front. Neuroendocrinol. 52, 22–28. https://doi.org/10.1016/j.yfrne.2018.06.004.

Lucas, R.J., Douglas, R.H., Foster, R.G., 2001. Characterization of an ocular photopigment capable of driving pupillary constriction in mice. Nat. Neurosci. 4, 621–626. https://doi.org/10.1038/88443.

Lucas, R.J., Hattar, S., Takao, M., Berson, D.M., Foster, R.G., Yau, K.W., 2003. Diminished pupillary light reflex at high irradiances in melanopsin-knockout mice. Science 299, 245–247. https://doi.org/10.1126/science.1077293.

Meltzer, E., Sguigna, P.V., Subei, A., Beh, S., Kildebeck, E., Conger, D., Conger, A., Lucero, M., Frohman, B.S., Frohman, A.N., Saidha, S., Galetta, S., Calabresi, P.A., Rennaker, R., Frohman, T.C., Kardon, R.H., Balcer, L.J., Frohman, E.M., 2017. Retinal architecture and melanopsin-mediated pupillary response characteristics: a putative pathophysiologic signature for the retino-hypothalamic tract in multiple sclerosis. JAMA Neurol 74, 574–582. https://doi.org/10.1001/jamaneurol.2016.5131.

Morin, L.P., Studholme, K.M., 2014. Retinofugal projections in the mouse. J. Comp. Neurol. 522, 3733–3753. https://doi.org/10.1002/cne.23635.

Moura, A.L., Nagy, B.V., La Morgia, C., Barboni, P., Oliveira, A.G., Salomão, S.R., Berezovsky, A., de Moraes-Filho, M.N., Chicani, C.F., Belfort Jr., R., Carelli, V., Sadun, A.A., Hood, D.C., Ventura, D.F., 2013. The pupil light reflex in Leber's

hereditary optic neuropathy: evidence for preservation of melanopsin-expressing retinal ganglion cells. Invest. Ophthalmol. Vis. Sci. 54, 4471–4477. https://doi.org/10.1167/iovs.12-11137.

Murakami, N., Kawano, T., Nakahara, K., Nasu, T., Shiota, K., 2001. Effect of melatonin on circadian rhythm, locomotor activity and body temperature in the intact house sparrow, Japanese quail and owl. Brain Res. 889 (1–2), 220–224. https://doi.org/10.1016/s0006-8993(00)03205-4.

Nadal Nicolás, F.M., Jiménez-López, M., Salinas-Navarro, M., Sobrado-Calvo, P., Alburquerque-Béjar, J.J., Vidal-Sanz, M., Agudo-Barriuso, M., 2012. Whole number, distribution and co-expression of brn3 transcription factors in retinal ganglion cells of adult albino and pigmented rats. PloS One 7, e49830. https://doi.org/10.1371/journal.pone.0049830.

Najafi, M.R., Toghianifar, N., Etemadifar, M., Haghighi, S., Maghzi, A.H., Akbari, M., 2013. Circadian rhythm sleep disorders in patients with multiple sclerosis and its association with fatigue: a case-control study. J. Res. Med. Sci. 18, S71–S73.

Obara, E.A., Hannibal, J., Heegaard, S., Fahrenkrug, J., 2016. Loss of melanopsin-expressing retinal ganglion cells in severely staged glaucoma patients. Invest. Ophthalmol. Vis. Sci. 57, 4661–4667. https://doi.org/10.1167/iovs.16-19997.

Panda, S., Provencio, I., Tu, D.C., Pires, S.S., Rollag, M.D., Castrucci, A.M., Pletcher, M. T., Sato, T.K., Wiltshire, T., Andahazy, M., Kay, S.A., Van Gelder, R.N., Hogenesch, J. B., 2003. Melanopsin is required for non-image forming photic responses in blind mice. Science 301, 525–527. https://doi.org/10.1126/science.1086179.

Pau, D., Al Zubidi, N., Yalamanchili, S., Plant, G.T., Lee, A.G., 2011. Optic neuritis. Eye 25, 833–842. https://doi.org/10.1038/eye.2011.81.

Paxinos, G., Watson, C., 1997. The Rat Brain in Stereotaxic Coordinates. Elsevier, Amsterdam.

Pérez-Rico, C., de la Villa, P., Arribas-Gómez, I., Blanco, R., 2010. Evaluation of functional integrity of the retinohypothalamic tract in advanced glaucoma using multifocal electroretinography and light-induced melatonin suppression. Exp. Eye Res. 91, 578–583. https://doi.org/10.1016/j.exer.2010.07.012.

Pfeffer, M., Korf, H.W., Wicht, H., 2018. Synchronizing effects of melatonin on diurnal and circadian rhythms. Gen. Comp. Endocrinol. 258, 215–221. https://doi.org/10.1016/j.ygcen.2017.05.013.

Richter, P., Wilhelm, H., Peters, T., Luedtke, H., Kurtenbach, A., Jaegle, H., Wilhelm, B., 2017. The diagnostic accuracy of chromatic pupillary light responses in diseases of the outer and inner retina. Graefes Arch. Clin. Exp. Ophthalmol. 255, 519–527. https://doi.org/10.1007/s00417-016-3496-6.

Robinson, G.A., Madison, R.D., 2004. Axotomized mouse retinal ganglion cells containing melanopsin show enhanced survival, but not enhanced axon regrowth into a peripheral nerve graft. Vis. Res. 44, 2667–2674. https://doi.org/10.1016/j.visres.2004.06.010.

Sánchez-Migallón, M.C., Valiente-Soriano, F.J., Nadal-Nicolás, F.M., Di Pierdomenico, J., Vidal-Sanz, M., Agudo-Barriuso, M., 2018. Survival of melanopsin expressing retinal ganglion cells long term after optic nerve trauma in mice. Exp. Eye Res. 174, 93–97. https://doi.org/10.1016/j.exer.2018.05.029.

Sande, P.H., Fernandez, D.C., Aldana Marcos, H.J., Chianelli, M.S., Aisemberg, J., Silberman, D.M., Sáenz, D.A., Rosenstein, R.E., 2008. Therapeutic effect of melatonin in experimental uveitis. Am. J. Pathol. 173, 1702–1713. https://doi.org/10.2353/ajpath.2008.080518.

Smith, R.E., Tournier, J.D., Calamante, F., Connelly, A., 2013. SIFT: spherical-deconvolution informed filtering of tractograms. Neuroimage 67, 298–312. https://doi.org/10.1016/j.neuroimage.2012.11.049.

Terrón, M.P., Delgado-Adámez, J., Pariente, J.A., Barriga, C., Paredes, S.D., Rodríguez, A.B., 2013. Melatonin reduces body weight gain and increases nocturnal activity in male Wistar rats. Physiol. Behav. 118, 8–13. https://doi.org/10.1016/j.physbeh.2013.04.006.

Toosy, A.T., Mason, D.F., Miller, D.H., 2014. Optic neuritis. Lancet Neurol. 13, 83–99. https://doi.org/10.1016/S1474-4422(13)70259-X.

Tournier, J.D., Calamante, F., Gadian, D.G., Connelly, A., 2004. Direct estimation of the fiber orientation density function from diffusion-weighted MRI data using spherical deconvolution. Neuroimage 23, 1176–1185. https://doi.org/10.1016/j.neuroimage.2004.07.037.

Türkoğlu, R., Benbir, G., Özyurt, S., Arsoy, E., Akbayır, E., Turan, S., Karadeniz, D., Yılmaz, V., Gencer, M., Tüzün, E., 2020. Sleep disturbance and cognitive decline in multiple sclerosis patients with isolated optic neuritis as the first demyelinating event. Int. Ophthalmol. 40, 151–158. https://doi: 10.1007/s10792-019-01157-x.

Tustison, N.J., Avants, B.B., Cook, P.A., Zheng, Y., Egan, A., Yushkevich, P.A., Gee, J.C., 2010. N4ITK: improved N3 bias correction. IEEE Trans. Med. Imag. 29, 1310–1320. https://doi.org/10.1109/TMI.2010.2046908.

Touitou, Y., Bogdan, A., 2007. Promoting adjustment of the sleep-wake cycle by chronobiotics. Physiol. Behav. 90, 294–300. https://doi.org/10.1016/j.physbeh.2006.09.001.

van Geijlswijk, I.M., Korzilius, H.P., Smits, M.G., 2010. The use of exogenous melatonin in delayed sleep phase disorder: a meta-analysis. Sleep 33, 1605–1614. https://doi.org/10.1093/sleep/33.12.1605.

Veraart, J., Novikov, D.S., Christiaens, D., Ades-Aron, B., Sijbers, J., Fieremans, E., 2016. Denoising of diffusion MRI using random matrix theory. Neuroimage 142, 394–406. https://doi.org/10.1016/j.neuroimage.2016.08.016.

Wirz-Justice, A., Armstrong, S.M., 1996. Melatonin: nature's soporific? J. Sleep Res. 5, 137–141.

Zisapel, N., 2018. New perspectives on the role of melatonin in human sleep, circadian rhythms and their regulation. Br. J. Pharmacol. 175, 3190–3199. https://doi.org/10.1111/bph.14116.